ANALYTICAL SCIENCES SEPTEMBER 2017, VOL. 33

Original Papers

Electrochemical Detection of Hydroxylamine *via* Au-Pt Alloy Nanoparticle-modified Single-walled Carbon Nanotube Electrodes

Yanfang Geng, Euna Ko, Van-Khue Tran, Woo Sung Chung, Chan Ho Park, Min Ki Kim, Ga Hyun Jin, and Gi Hun Seong†

Department of Bionano Engineering, Hanyang University, Ansan, 425-791, South Korea

In the present study, we developed an electrochemical sensor for highly sensitive detection of hydroxylamine using Au-Pt alloy nanoparticles. Au-Pt alloy nanoparticles were electrochemically deposited on a working electrode made of single-walled carbon nanotubes. The framework composition in the Au-Pt alloy nanoparticle was easily controlled by adjusting the Au^{3+}:Pt^{4+} composition ratio in the precursor solution. Morphological and chemical characterizations of the resulting Au-Pt alloy nanoparticles were performed using field emission scanning electron microscopy, X-ray diffraction, and energy dispersion X-ray spectroscopy. When the Au^{3+}:Pt^{4+} ratio in the precursor solution was 1:5, the ratio of Au:Pt atom in alloy nanoparticle was about 6:4. $Au_{60}Pt_{40}$ alloy nanoparticles were found to have the optimum synthetic ratio for hydroxylamine detection. The electrocatalytic performance of Au-Pt alloy nanoparticles in the presence of hydroxylamine was also characterized using cyclic voltammetry, differential pulse voltammetry, and chronoamperometry. In the chronoamperometric detection of hydroxylamine, the sensor exhibited a detection limit of 0.80 μM (S/N = 3) and a high sensitivity of 184 μA mM^{-1} cm^{-2}. Moreover, the amperometric response of the sensor in 1 mM hydroxylamine was stable for a long time (450 s). Long-term stability tests showed that the current responses to hydroxylamine were 96, 91 and 85% of the initial signal value after storage for 5, 10, and 20 days, respectively.

Keywords Au-Pt alloy nanoparticles, single-walled carbon nanotube, hydroxylamine, electrochemical sensor, electrocatalysis

(Received February 10, 2017; Accepted April 26, 2017; Published September 10, 2017)

Introduction

Hydroxylamine (NH_2OH), an oxygenated derivative of ammonia, is known to be a potent reducing agent and is identified as an important mediator in the nitrogen cycle and nitrous oxide formation.[1] It is commonly used as a raw material in industrial and pharmaceutical processes, where some hydroxylamine derivatives are used to make anticancer drugs.[2,3] Furthermore, hydroxylamine is also well-known as a mutation agent, and it can be toxic to humans, animals, and plants, even at low concentrations.[4] Therefore, reliable, reproducible, and highly sensitive detection of hydroxylamine at low levels is of tremendous importance in industry, environmental testing, clinical diagnostics, and biological processing. Many methods have been developed for hydroxylamine detection, such as gas chromatography,[5] spectrometry,[6] and electrochemical detection.[7–10] Compared to the other methods, the electrochemical method has various advantages such as low detection limit, fast response, low cost, and portability.[11–13]

Most bare electrodes used for the electrochemical detection of hydroxylamine have a number of limitations (*e.g.*, low selectivity and reproducibility, high overpotential, and low stability over a wide range of solution compositions). However, using nanoparticles as redox-active materials offers significant advantages in the development of electrochemical sensors. Recently, bimetallic nanoparticles have become important for improving the catalytic properties of monometallic nanoparticles. The improvements derived from the combination of two metal elements into bimetallic nanoparticles can be attributed to synergistic effects.[14] In particular, Au-Pt alloy nanoparticles have been extensively researched because the Au-Pt bimetallic system has greater catalytic activity and enhanced functionalities than pure Pt or Au.[15] However, it is challenging to synthesize single-phase Au-Pt alloys because they are immiscible in the bulk.[16] The general method to obtain Au-Pt alloy nanoparticles involves reducing the respective metal salt precursors simultaneously with the help of reducing agents. Here, the electrochemical method was used to obtain Au-Pt bimetallic nanoparticles, which can be used in exciting technological applications such as electrocatalysts, selective oxidants, sensors, and dehydrogenation catalysts.[17-19]

Traditional electrodes, such as glassy carbon, gold, and ITO are commonly used, but they are difficult to fabricate, limited in sensor design, and expensive to manufacture. In contrast, single-walled carbon nanotubes (SWCNT) are becoming popular electrode materials due to their unique properties, including their large electrode surface area, fast electron transfer rate, good mechanical strength, and chemical stability. Therefore, SWCNTs have been used as electrode materials in applications of electronics, catalysis, and sensing.[20,21] Our recent studies have demonstrated that SWCNT electrodes have strong electrocatalytic activity when modified with metal

† To whom correspondence should be addressed.
E-mail: ghseong@hanyang.ac.kr

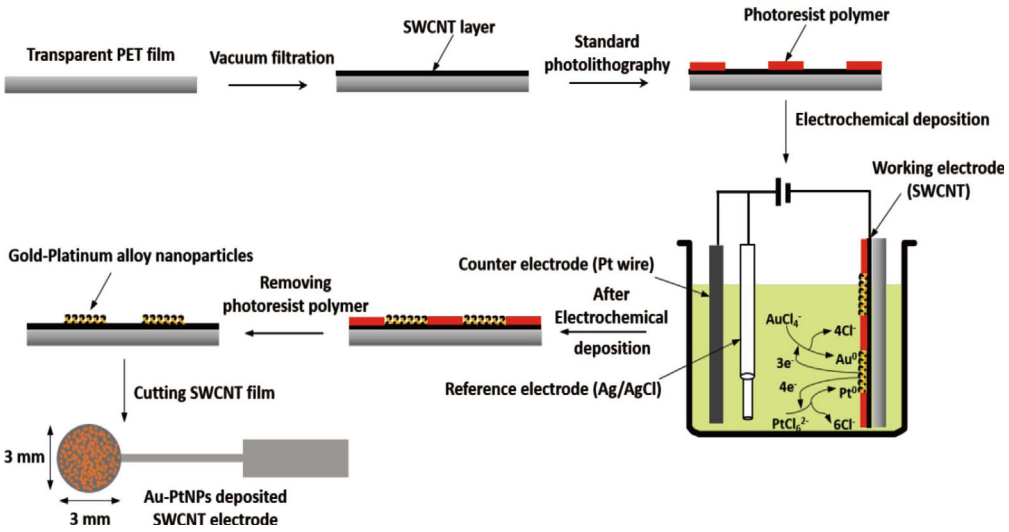

Fig. 1 Schematic illustration of the fabrication process for Au-Pt alloy nanoparticles on a SWCNT electrode using an electrochemical deposition method.

nanoparticles such as gold,[22] silver,[23] platinum,[24] and palladium.[25] The remarkable properties of the Au-Pt alloy nanoparticles and SWCNT electrodes motivated us to design alloy nanoparticle-modified SWCNT sensors for the electrochemical detection of hydroxylamine.

In this work, Au-Pt alloy nanoparticles were deposited electrochemically on a SWCNT electrode and were used to detect hydroxylamine by cyclic voltammetry, differential pulse voltammetry, and amperometry. Electrochemical characterization showed that the Au-Pt bimetallic system had greater electrocatalytic activity toward hydroxylamine compared to monometallic Pt or Au nanoparticles. Moreover, the developed hydroxylamine sensor exhibited high sensitivity, good stability, and rapid response.

Experimental

Materials

An SWCNT solution (0.3 mg/mL) was obtained from Top Nanosys Co. (Sung Nam, South Korea). Gold(III) chloride trihydrate (99.99%), chloroplatinic acid hexahydrate (37.50%), hydroxylamine solution (99.99%), sulfuric acid (95 – 98%), and phosphate buffer components were purchased from Sigma-Aldrich (St. Louis, MO). Photoresist (AZ4620) was obtained from Clariant Corporation (Somerville, NJ, USA). Tetrahydrofuran (THF) and ethanol were purchased from Samchun Pure Chemical Co. (Seoul, South Korea). All other chemicals were of analytical grade and aqueous solutions were prepared with deionized (DI) water. Morphologies of Au-Pt alloy nanoparticles were investigated by using field emission scanning electron microscopy (FE-SEM, Hitachi Co., Ltd., S-4800, Japan) at an accelerating voltage of 15 kV. X-ray diffraction (XRD) was carried out using a D/MAX-2500/PC instrument (Rigaku Corp., Japan) with Cu $K\alpha$ radiation λ = 0.15406 nm at a scanning rate of 2°/min.

Preparation of SWCNT electrode

Homogeneous and flexible SWCNT films were fabricated by using the vacuum filtration method. First, sonication of the SWCNT solution was performed for 1 h followed by 10 min of centrifugation at 12000 rpm. Next, the pre-suspended solution was diluted by a factor of 100 using DI water, and it was then filtered through an anodic aluminum oxide membrane with a 0.2 µm pore size. The alumina membrane under the SWCNT thin layer was easily removed in a 3 M NaOH solution. After adjusting the solution to neutral pH by using DI water, the SWCNT thin layer was directly transferred to a flexible, transparent PET film.

Fabrication of Au-Pt alloy nanoparticles on SWCNT electrodes

The procedure for fabrication of Au-Pt alloy nanoparticles on SWCNT electrodes was performed as described in our previous publication with some modifications (Fig. 1).[26,27] Briefly, a standard photolithography process was used to generate a photoresist polymer template (AZ4620) on the SWCNT electrode. Au-Pt alloy nanoparticles were electrochemically deposited on the pre-patterned SWCNT electrode using 1 mM $HAuCl_4$ and 5 mM H_2PtCl_6 as precursors. Cyclic voltammetry was used for repeated potential scanning from –1 to 0.6 V, and chronocoulommetry was conducted at a potential of –0.5 V (*vs.* Ag/AgCl). A clean platinum wire and Ag/AgCl (saturated in 3 M NaCl) were used as the counter and reference electrode, respectively. The resulting SWCNT electrodes were then immersed in the THF solution to completely remove the photoresist polymer from the SWCNT electrodes. After removing the photoresist polymer, each area deposited with Au-Pt alloy nanoparticles was cut and used as electrode platforms to detect hydroxylamine. The area of each working electrode was 0.07 cm^2.

Electrocatalytic characteristics and detection of hydroxylamine

Electrochemical measurements were performed with a CHI660C electrochemical analyzer (CH Instruments Inc., USA). A three-electrode configuration was employed, in which the Au-Pt alloy nanoparticle-modified SWCNT working electrode was placed into a solution with a clean platinum wire counter electrode and an Ag/AgCl (saturated in 3 M NaCl) reference electrode. A 0.1 M phosphate-buffered saline (PBS, pH 7.4) solution was used to support the electrolytes in all measurements. Each cyclic voltammetry was in a known concentration of hydroxylamine solution with a scan rate of 20 mV s^{-1}.

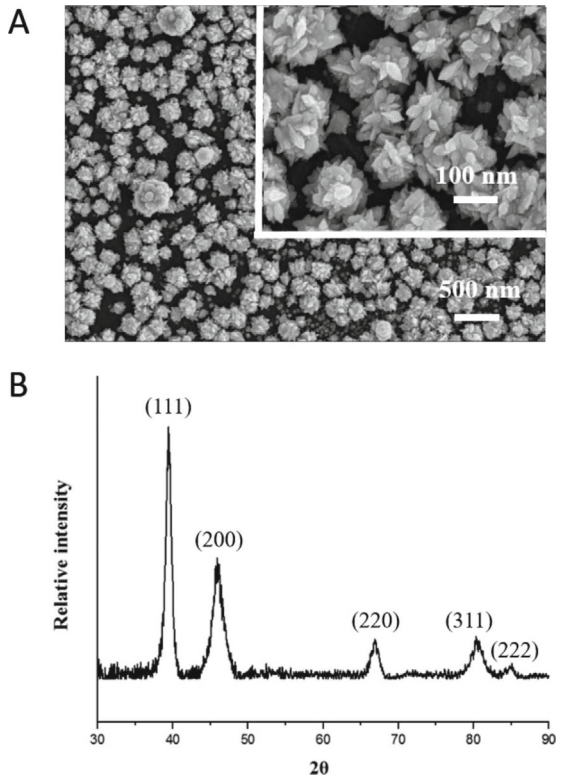

Fig. 2 (A) FE-SEM image of the Au-Pt alloy nanoparticles. The inset shows high magnification of alloy nanoparticles. (B) XRD pattern of Au-Pt alloy nanoparticles on a SWCNT electrode.

In differential pulse voltammetry, the following optimized parameters were used: $E_{initial}$, –0.3 V; E_{final}, +0.4 V; step, 0.004 V; amplitude, 0.05 V; pulse width, 0.2 s; pulse period, 0.5 s. Amperometric measurements of hydroxylamine were performed at the desired potential of 0.2 V for electro-oxidation.

Results and Discussion

Characterization of Au-Pt alloy nanoparticles on SWCNT electrodes

Homogeneous SWCNT films were prepared on flexible, transparent PET substrates with a thickness of ~100 nm, and their average resistivity and transparency were 350 Ω sq^{-1} and 80%, respectively. The SWCNT films exhibited high flexibility with negligible change in resistivity upon comparatively large bending deformation. These good properties of the SWCNT film ensure that it can be used as a conductive substrate for electrodeposition of nanoparticles and can provide a rapid electron transfer path in electrochemical processes.[23,28] Moreover, well-defined photoresist polymer patterns on the SWCNT film made using the photolithography method provide excellent conditions for the electrochemical deposition of nanoparticles on the SWCNT surface due to the high electric field strength induced by the features of the pattern.[29]

Figure 2A shows the FE-SEM image of the as-prepared Au-Pt alloy nanoparticles on the SWCNT electrode after the electrochemical deposition process. The Au-Pt alloy nanoparticles were highly crystalline and homogenously distributed, and the diameters of the alloy nanoparticles were in the range of 100 – 300 nm. The formation of the Au-Pt alloy nanoparticles on the SWCNT films was mainly controlled by the growth of nuclei.[30-32] The Au^{3+} ions are first reduced on the SWCNT film, and the newly formed Au nuclei work as a catalyst by promoting the reduction of $PtCl6^{2-}$ ions on the Au nuclei. The electrochemical deposition of Au-Pt alloy nanoparticles on the SWCNT film was affected by both diffusion shield effects and kinetic control. The morphology of the nanoparticles on the SWCNT film may affect the electrochemical properties of the electrodes.

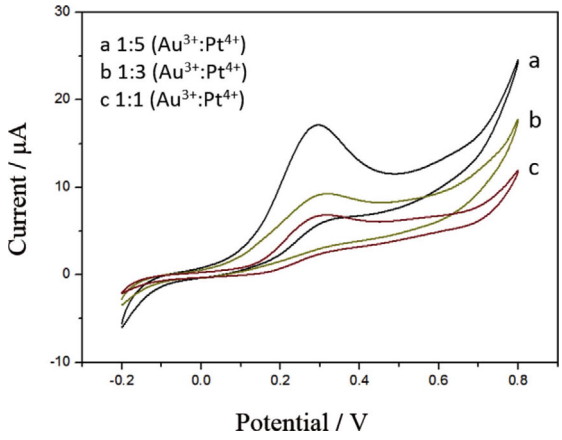

Fig. 3 Cyclic voltammograms of 1 mM hydroxylamine in 0.1 M PBS (pH 7.4) for the Au-Pt alloy nanoparticles prepared with different compositional ratios. The scan rate was 20 mV s^{-1}.

The XRD pattern of the Au-Pt alloy nanoparticles is significant in that the alloy nanoparticles have a face-centered cubic (fcc) crystal structure (Fig. 2B). Five peaks derived from deposited samples were clearly observed at 39.4°, 45.9°, 66.9°, 80.5°, and 84.8°, which correspond to the orientations along (111), (200), (220), (311), and (222) directions of the fcc crystal structure, respectively. Compared with Au alone, the (111) peaks obviously shifted to a higher 2θ angle. These peaks for Au-Pt alloy nanoparticles were observed between the peaks of pure Au and pure Pt as a single peak, revealing single-phase alloy fcc-type nanostructures rather than a mixture of monometals or a core-shell structure.[33,34]

Optimization of Au/Pt synthetic ratio for hydroxylamine detection

The synergistic catalysis of bimetallic alloy nanoparticles depends on the nanoscale size, composition, and surface properties.[35] To investigate the effect of the composition of the alloy nanoparticle on electrochemical hydroxylamine oxidation, cyclic voltammetry measurements were performed in 1 mM hydroxylamine (Fig. 3). Alloy nanoparticles with different compositional ratios were fabricated by changing the Au^{3+}:Pt^{4+} ratio in the precursor solutions. Increasing the Pt content in the Au-Pt alloy nanoparticles led to an increase in peak current because plenty of active Pt atoms were present. The enhancement in electrocatalytic activity has been attributed to the synergistic effect of the surface electronic states on the effective atomic coordination number.[14] In particular, it has been found that Pt in Au-Pt alloy nanoparticles plays an important role in enhancing catalytic activity.

When the Au^{3+}:Pt^{4+} ratio in the precursor solution was 1:5, the ratio of Au:Pt atom in the alloy nanoparticle was about 6:4. This was confirmed by energy dispersion X-ray spectroscopy (EDX) elemental mapping of Au-Pt alloy nanoparticles on the SWCNT electrode (Fig. 4). In the fabricated Au-Pt alloy nanoparticles, both Au and Pt atoms were distributed homogeneously throughout the structure. The elemental

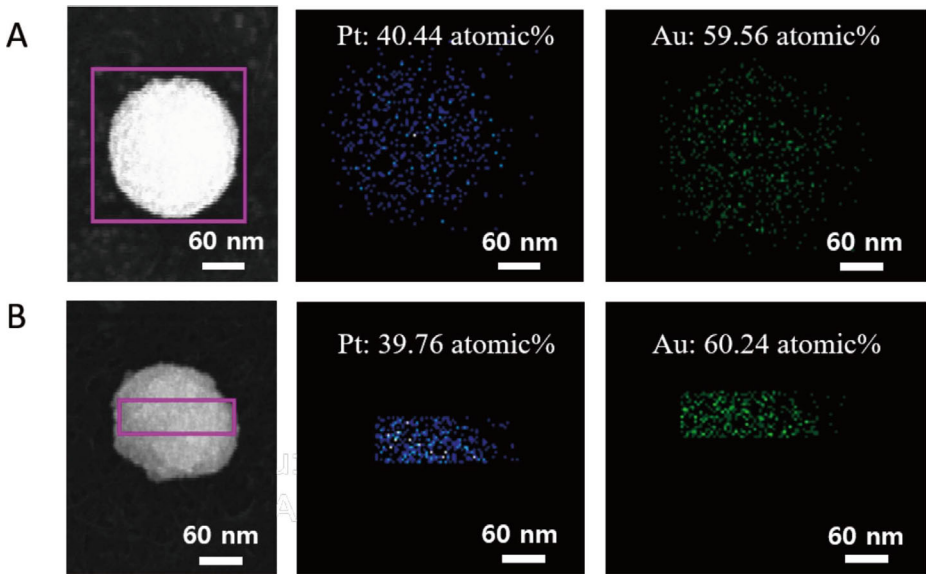

Fig. 4 Elemental mappings for Au-Pt alloy nanoparticles by EDX. Each Au-Pt alloy nanoparticle shown in (A) and (B) was fabricated under the same conditions (the Au^{3+}:Pt^{4+} ratio in the precursor solution was 1:5).

composition analyses showed that the atomic percentages of Au and Pt were 60 atomic% and 40 atomic%, respectively. Theoretically, an Au:Pt atom ratio of 5:5 was predicted to be the most active bimetallic composition.[36] However, in this study, the signal current of the $Au_{50}Pt_{50}$ alloy nanoparticle showed a larger decrease after two weeks than that of the $Au_{60}Pt_{40}$ alloy nanoparticle. Therefore, the $Au_{60}Pt_{40}$ alloy nanoparticle was found to be the optimum synthetic ratio for hydroxylamine detection.

Electrochemical behavior of hydroxylamine by Au-Pt alloy nanoparticles

To show the enhancement in electrocatalytic activity caused by the Au-Pt alloy nanoparticles, hydroxylamine oxidation by cyclic voltammetry was investigated on different electrode surfaces. Figure 5A shows the cyclic voltammetry responses for the electrochemical oxidation of 1 mM hydroxylamine on four different electrodes made of: pristine SWCNTs (curve a), Au nanoparticle-SWCNTs (curve b), Pt nanoparticle-SWCNTs (curve c), and Au-Pt alloy nanoparticle-SWCNTs (curve d). No redox peaks were observed for the pristine SWCNT electrode over a wide range of potentials. However, the Au-Pt alloy nanoparticle-SWCNT electrode exhibited the highest anodic peak compared to those observed for the Pt nanoparticle-SWCNT and Au nanoparticle-SWCNT electrodes. This large peak current during the oxidation of hydroxylamine was attributed to the synergic effect of the Au and Pt bimetallic nanoparticles.[14] As shown in the EDX elemental mappings, nanoscale Pt, which plays an important role in the oxidation of hydroxylamine, was distributed in the alloy particle, resulting in a larger active surface area than pure Pt particles. Hydroxylamine oxidation peaks on the Au-Pt alloy nanoparticle-SWCNT electrode occurred around 0.3 V, which was similar to the value observed for the Pt nanoparticle-SWCNT electrode. The anodic peak of hydroxylamine is broad, which suggests a mechanistically complex oxidation process that includes: absorption of hydroxylamine on the Au-Pt alloy nanoparticles, formation of an intermediate hydroxylamine layer, and oxidation of intermediate compounds through the $2e^-$ oxidation pathway.[37,38]

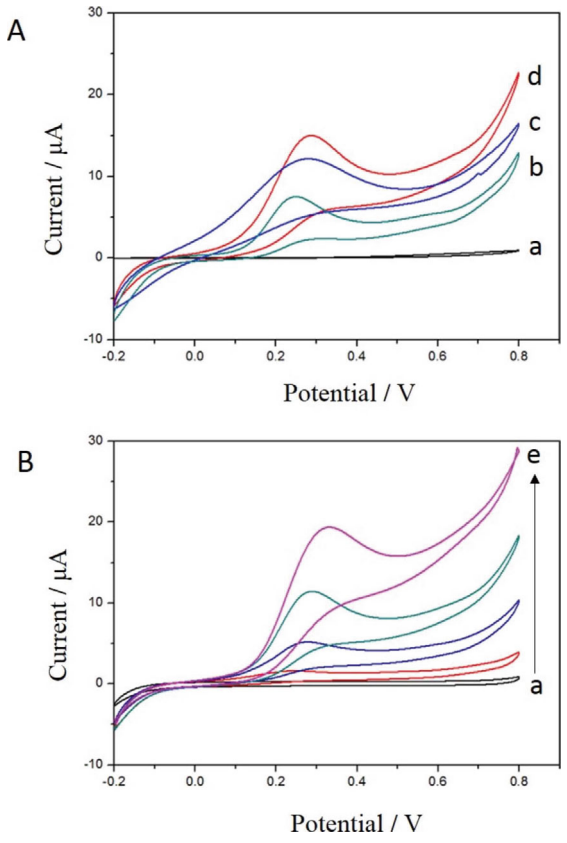

Fig. 5 (A) Cyclic voltammograms for the oxidation of 1 mM hydroxylamine for (a) pristine SWCNTs, (b) Au nanoparticle-SWCNTs, (c) Pt nanoparticle-SWCNTs, and (d) Au-Pt alloy nanoparticle-SWCNT electrodes in 0.1 M PBS (pH 7.4) at a scan rate of 20 mV s^{-1}. The area of each working electrode was 0.07 cm^2. (B) Cyclic voltammograms at different hydroxylamine concentrations using the Au-Pt alloy nanoparticle-SWCNT electrode. The hydroxylamine concentrations from (a) to (e) were 0, 0.1, 0.5, 1.0, and 2.0 mM, respectively.

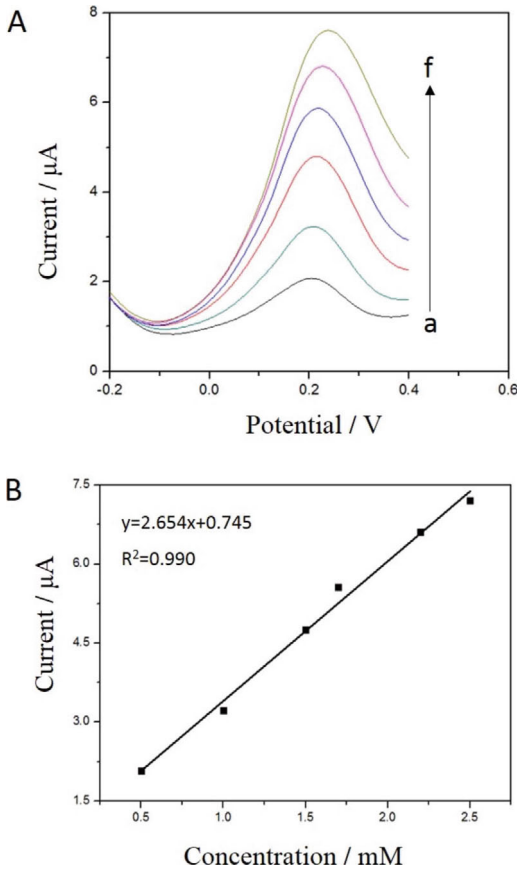

Fig. 6 (A) Differential pulse voltammetric responses of various hydroxylamine concentrations on the Au-Pt alloy nanoparticle-SWCNT electrode. The hydroxylamine concentrations from (a) to (f) were 0.5, 1.0, 1.5, 1.7, 2.2, and 2.5 mM, respectively. (B) The calibration curve shows the linear relationship between the oxidation peak current and concentration.

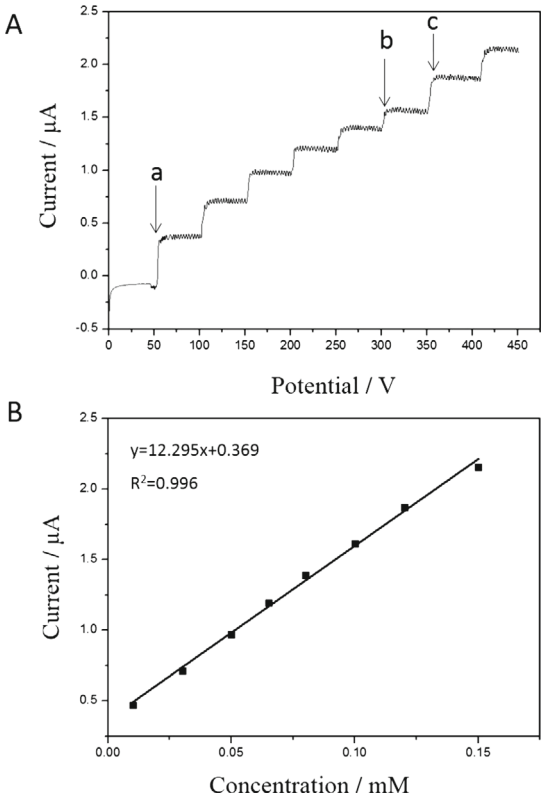

Fig. 7 (A) Amperometric response of the Au-Pt alloy nanoparticle-SWCNT electrode in a hydroxylamine solution at a potential of 0.2 V. (a, b) 50 mL and upon the addition of (c) 100 mL of 1 mM hydroxylamine to the 0.1 M PBS (pH 7.4) solution. (B) The calibration plot for the signal and concentration of hydroxylamine solution.

Cyclic voltammetry, differential pulse voltammetry, and chronoamperometry for the detection of hydroxylamine on Au-Pt alloy nanoparticle-SWCNT sensors

The electrochemical detection of hydroxylamine by Au-Pt alloy nanoparticle-SWCNT sensors was performed in different concentrations of hydroxylamine in 0.1 M PBS (pH 7.4) by the cyclic voltammetry technique (Fig. 5B). A possible electro-oxidation mechanism for hydroxylamine is expressed in the following reaction:

$$2NH_2OH \longrightarrow N_2O + H_2O + 4H^+ + 4e^-$$

The current response had a linear correlation with the hydroxylamine concentration. The current changed linearly with concentration for concentrations ranging from 100 μM to 2 mM. The sensitivity and detection limit were determined to be 56 μA mM^{-1} cm^{-2} and 46 μM, respectively.

To obtain better performance in the detection of hydroxylamine, we also employed a differential pulse voltammetry technique. Pulse voltammetric techniques have been widely used due to their advantageous characteristics, which include low detection limit, minimization of capacitive current, reduction of background currents, and ability to sample the current immediately before the potential is changed. Figure 6A shows the differential pulse voltammetric responses of different hydroxylamine concentrations in 0.1 M PBS (pH 7.4). A well-defined oxidation peak at ~200 mV was observed for each hydroxylamine concentration on the Au-Pt alloy nanoparticle-SWCNT sensor. Figure 6B shows a good linear relationship between the current response and hydroxylamine concentrations ranging from 0.5 to 2.5 mM. The linear regression equation (n = 5) was $i_{pa} = 2.654c + 0.745$ (i_{pa}: μA, c: mM) with a correlation coefficient of $R^2 = 0.990$, and the detection limit was determined to be as low as 15 μM (S/N = 3). The Au-Pt alloy nanoparticle-SWCNT sensor showed higher sensitivity (72 μA mM^{-1} cm^{-2}) in the linear range than that that observed using the cyclic voltammetry technique.

Chronoamperometry was also used to study the electrochemical behavior of various hydroxylamine concentrations using Au-Pt alloy nanoparticle-SWCNT sensors. The amperometric responses for hydroxylamine electro-oxidation and calibration plots are shown in Fig. 7. To obtain a steady-state response, a working potential of 0.2 V (*vs.* Ag/AgCl) was applied with each addition of hydroxylamine into a stirred supporting electrolyte solution. As depicted in Fig. 7A, rapid and stable current responses were observed within 3 s of changing the hydroxylamine concentration. This behavior was attributed to the good electrocatalytic properties of the Au-Pt alloy nanoparticles. A clear increase in the oxidation current upon the successive addition of hydroxylamine was also observed. The resulting calibration curve for hydroxylamine on the Au-Pt alloy nanoparticles-SWCNT sensor displayed good linearity for concentrations ranging from 10 to 150 μM with a correlation coefficient of $R^2 = 0.996$ (Fig. 7B). The detection limit, which was three times the standard deviation of the blank signal/slope, was 0.80 μM, and the evaluated sensitivity was 184 μA mM^{-1} cm^{-2}.

Stability and reproducibility

The stability of the fabricated hydroxylamine sensor was examined by monitoring its current response after successive cycling (for 200 cycles) in the potential range of –0.2 to +0.8 V in a 0.1 M PBS buffer (pH 7.4) including 1 mM hydroxylamine. The oxidation peak current of hydroxylamine retained 90% of its initial value, which indicates that hydroxylamine and its oxidation products had an insignificant fouling effect on the Au-Pt alloy nanoparticle-SWCNT electrodes. Moreover, the amperometric response of the sensor in 1 mM hydroxylamine was stable for a long time (450 s). The reproducibility of our fabricated sensor was also investigated by performing measurements with five different sensors in the same 1 mM hydroxylamine solution. The relative standard deviation (RSD) for detecting hydroxylamine was 1.1%, indicating that the sensors can be reliably reproduced. The long-term stability of the Au-Pt alloy nanoparticle-SWCNT sensors was evaluated by taking measurements over a 20-day period. The current responses to 1 mM hydroxylamine were 96, 91 and 85% of the initial signal value after storage for 5, 10, and 20 days, respectively.

Conclusions

A highly sensitive, stable, and rapid-response electrochemical sensor was developed to detect hydroxylamine by electrochemically co-depositing Au and Pt bimetallic ions on SWCNT electrodes. The sensor fabrication process was simple, and the Au-Pt alloy nanoparticle-SWCNT sensor showed excellent electrocatalytic performance toward the oxidation of hydroxylamine in 0.1 M PBS (PH 7.4) due to the synergistic effect of the Au-Pt alloy nanostructure. The developed sensor showed a good linear range of hydroxylamine detection ranging from 10 to 150 μM ($R^2 = 0.996$) with a detection limit of 0.80 μM. Moreover, the fabricated hydroxylamine sensor exhibited good stability and reproducibility for hydroxylamine oxidation. We expect that patterning alloy nanoparticles onto the SWCNT electrode using this technique can be used to create promising electroanalytical platforms for biochemical sensing in various fields and may also be extended to other alloy nanoparticles.

Acknowledgements

This research was supported by the Basic Science Research Program through the National Research Foundation of Korea (NRF) funded by the Ministry of Science, ICT & Future Planning (2008-0061891).

References

1. T. Hofman and H. Lees, *Biochem. J.*, **1953**, *54*, 579.
2. A. Leroux, C. Junien, J.-C. Kaplan, and J. Bamberger, *Nature*, **1975**, *258*, 619.
3. G. Choudhary and H. Hansen, *Chemosphere*, **1998**, *37*, 801.
4. R. P. Smith and W. R. Layne, *J. Pharmacol. Exp. Ther.*, **1969**, *165*, 30.
5. J. H. Butler and L. I. Gordon, *Mar. Chem.*, **1986**, *19*, 229.
6. G. C. M. Bourke, G. Stedman, and A. P. Wade, *Anal. Chim. Acta*, **1983**, *153*, 277.
7. C. Zhao and J. Song, *Anal. Chim. Acta*, **2001**, *434*, 261.
8. R. Christova, M. Ivanova, and M. Novkirishka, *Anal. Chim. Acta*, **1976**, *85*, 301.
9. D. R. Canterford, *Anal. Chim. Acta*, **1978**, *98*, 205.
10. S. Ikeda and J. Motonaka, *Anal. Chim. Acta*, **1977**, *90*, 257.
11. C. Zhang, G. Wang, M. Liu, Y. Feng, Z. Zhang, and B. Fang, *Electrochim. Acta*, **2010**, *55*, 2835.
12. H. M. Moghaddam, H. Beitollahi, S. Tajik, M. Malakootian, and H. K. Maleh, *Environ. Monit. Assess.*, **2014**, *186*, 7431.
13. A. Safavi, Z. Shojaeifard, and M. Tohidi, *IEEE Sens. J.*, **2014**, *14*, 839.
14. A. K. Singh and Q. Xu, *ChemCatChem*, **2013**, *5*, 652.
15. Y. Luo, H. O. Seo, K.-D. Kim, M. J. Kim, W. S. Tai, M. Burkhart, and Y. D. Kim, *Catal. Lett.*, **2010**, *134*, 45.
16. R. Hultgren, P. D. Desai, D. T. Hawkins, M. Gleiser, and K. K. Kelley, "*Selected Values of the Thermodynamic Properties of Binary Alloys*", DTIC Document, **1973**.
17. M. Mirdamadi-Esfahani, M. Mostafavi, B. Keita, L. Nadjo, P. Kooyman, and H. Remita, *Gold Bull.*, **2010**, *43*, 49.
18. V. Abdelsayed, A. Aljarash, M. S. El-Shall, Z. A. Al Othman, and A. H. Alghamdi, *Chem. Mater.*, **2009**, *21*, 2825.
19. P. Hernández-Fernández, S. Rojas, P. Ocón, J. L. Gómez de la Fuente, J. San Fabián, J. Sanza, M. A. Peña, F. J. García-García, P. Terreros, and J. L. G. Fierro, *J. Phys. Chem. C*, **2007**, *111*, 2913.
20. K. Balasubramanian and M. Burghard, *Anal. Bioanal. Chem.*, **2006**, *385*, 452.
21. R. H. Baughman, A. A. Zakhidov, and W. A. de Heer, *Science*, **2002**, *297*, 787.
22. M.-P. N. Bui, X.-H. Pham, K. N. Han, C. A. Li, E. K. Lee, H. J. Chang, and G. H. Seong, *Electrochem. Commun.*, **2010**, *12*, 250.
23. M.-P. N. Bui, X.-H. Pham, K. N. Han, C. A. Li, Y. S. Kim, and G. H. Seong, *Sens. Actuators, B*, **2010**, *150*, 436.
24. C. A. Li, K. N. Han, M. P. N. Bui, X. H. Pham, M. H. Hong, M. Irfan, Y. S. Kim, and G. H. Seong, *J. Appl. Electrochem.*, **2011**, *41*, 1425.
25. X. H. Pham, M. P. NgocBui, C. A. Li, K. N. Han, and G. H. Seong, *Electroanalysis*, **2011**, *23*, 2087.
26. M.-P. N. Bui, S. Lee, K. N. Han, X.-H. Pham, C. A. Li, J. Choo, and G. H. Seong, *Chem. Commun.*, **2009**, 5549.
27. K. N. Han, C. A. Li, M.-P. N. Bui, and G. H. Seong, *Langmuir*, **2010**, *26*, 598.
28. K. N. Han, C. A. Li, M.-P. N. Bui, X.-H. Pham, and G. H. Seong, *Chem. Commun.*, **2011**, *47,* 938.
29. B. Yang, N. Lu, C. Huang, D. Qi, G. Shi, H. Xu, X. Chen, B. Dong, W. Song, B. Zhao, and L. Chi, *Langmuir*, **2009**, *25*, 55.
30. D. S. Kim, T. Lee, and K. E. Geckeler, *Angew. Chem., Int. Ed. Engl.*, **2005**, *45*, 104.
31. S. Guo, L. Wang, and E. Wang, *Chem. Commun.*, **2007**, 3163.
32. Y. Zilberman, U. Tisch, G. Shuster, W. Pisula, X. Feng, K. Müllen, and H. Haick, *Adv. Mater.*, **2010**, *22,* 4317.
33. H. Ataee-Esfahani, L. Wang, Y. Nemoto, and Y. Yamauchi, *Chem. Mater.*, **2010**, *22*, 6310.
34. H. Ataee-Esfahani, L. Wang, and Y. Yamauchi, *Chem. Commun.*, **2010**, *46*, 3684.
35. J. Wu, S. Shan, J. Luo, P. Joseph, V. Petkov, and C. J. Zhong, *ACS Appl. Mater. Interfaces*, **2015**, *7*, 25906.
36. W. Tang, L. Zhang, and G. Henkelman, *J. Phys. Chem. Lett.*, **2011**, *2*, 1328.
37. J. Li and X. Lin, *Sens. Actuators, B*, **2007**, *126*, 527.
38. M. Ebadi, *Electrochim. Acta*, **2003**, *48*, 4233.